Activation of Coq6p, a FAD Monooxygenase Involved in Coenzyme Q Biosynthesis by Adrenodoxin Reductase/Ferredoxin

Lucie Gonzalez, Samuel Chau-Duy Tam Vo, Bruno Faivre, Fabien Pierrel, Marc Fontecave, Djemel Hamdane, Murielle Lombard

ChemBioChem

Research Article
doi.org/10.1002/cbic.202300738

Chemistry Europe
European Chemical Societies Publishing

www.chembiochem.org

Activation of Coq6p, a FAD Monooxygenase Involved in Coenzyme Q Biosynthesis, by Adrenodoxin Reductase/Ferredoxin

Lucie Gonzalez,[a] Samuel Chau-Duy Tam Vo,[a, b] Bruno Faivre,[a] Fabien Pierrel,[c] Marc Fontecave,*[a] Djemel Hamdane,*[a, d] and Murielle Lombard*[a]

Adrenodoxin reductase (AdxR) plays a pivotal role in electron transfer, shuttling electrons between NADPH and iron/sulfur adrenodoxin proteins in mitochondria. This electron transport system is essential for P450 enzymes involved in various endogenous biomolecules biosynthesis. Here, we present an in-depth examination of the kinetics governing the reduction of human AdxR by NADH or NADPH. Our results highlight the efficiency of human AdxR when utilizing NADPH as a flavin reducing agent. Nevertheless, akin to related flavoenzymes such as cytochrome P450 reductase, we observe that low NADPH concentrations hinder flavin reduction due to intricate equilibrium reactions between the enzyme and its substrate/product. Remarkably, the presence of $MgCl_2$ suppresses this complex kinetic behavior by decreasing NADPH binding to oxidized AdxR, effectively transforming AdxR into a classical Michaelis-Menten enzyme. We propose that the addition of $MgCl_2$ may be adapted for studying the reductive half-reactions of other flavoenzymes with NADPH. Furthermore, *in vitro* experiments provide evidence that the reduction of the yeast flavin monooxygenase Coq6p relies on an electron transfer chain comprising NADPH-AdxR-Yah1p-Coq6p, where Yah1p shuttles electrons between AdxR and Coq6p. This discovery explains the previous *in vivo* observation that Yah1p and the AdxR homolog, Arh1p, are required for the biosynthesis of coenzyme Q in yeast.

Introduction

Coenzyme Q, a vital lipophilic quinone playing a pivotal role in the mitochondrial respiratory chain, undergoes a complex biosynthetic process requiring three distinct hydroxylation reactions at specific positions on its benzene ring, namely C1, C5 and C6.[1] While the eukaryotic enzyme Coq7 has been biochemically characterized as a non-heme di-iron cluster metalloenzyme receiving its electrons from NADH for the C6 hydroxylation,[2] the counterparts responsible for the C1 and C5, the other two enzymes responsible for the C1 and C5 hydroxylation have remained enigmatic, with limited biochemical investigations. Our research conducted in the yeast *Saccharomyces cerevisiae* has unveiled the involvement of a flavin monooxygenase, Coq6p, in the C5 hydroxylation process.[3] Furthermore, our genetics studies have indicated the essential role of Arh1p and Yah1p, the yeast homologs of human AdxR (adrenodoxin reductase) and of both Fdx1 and Fdx2 (ferredoxin) respectively, in facilitating Coq6p's activity.[4] However, the interplay between Arh1p-Yah1p and Coq6p has remained enigmatic. Indeed, like for other one-component class A flavin monooxygenases, the reduction of the FAD cofactor of Coq6p is expected to involve a hydride transfer from NAD(P)H.[5] During our efforts to get insights into the mechanism of Coq6p activation, namely the reduction of its FAD cofactor as a prerequisite for O_2 activation, and into the role of the adrenodoxin reductase/ferredoxin couple, we discovered that adrenodoxin reductase had an intriguing kinetics behavior. This led us to carry out a thorough biochemical kinetics study of the human adrenodoxin reductase (hAdxR, NADPH:adrenal ferredoxin oxidoreductase, EC 1.18.1.6). In this study one could not use Arh1p, the yeast adrenodoxin reductase, as we failed to express and purify it, in agreement with a previous observation from Lill and collaborators.[6] However, hAdxR which shares 65%

[a] Dr. L. Gonzalez, Dr. S. Chau-Duy Tam Vo, B. Faivre, Prof. M. Fontecave, Dr. D. Hamdane, Dr. M. Lombard
Laboratoire de Chimie des Processus Biologiques, Collège de France, Sorbonne Université, CNRS UMR8229, PSL Research University, Sorbonne Université, 11 place Marcelin Berthelot, 75 005 Paris, France
033-1-44-27-12-54
033-1-44-27-16-45
033-1-44-27-13-60
E-mail: murielle.lombard@college-de-france.fr
djemel.hamdane@college-de-france.fr
marc.fontecave@college-de-france.fr

[b] Dr. S. Chau-Duy Tam Vo
Broad Institute of MIT and Harvard, Cambridge, MA, USA

[c] Dr. F. Pierrel
Univ. Grenoble Alpes, CNRS, UMR 5525, VetAgro Sup, Grenoble INP, TIMC, 38000 Grenoble, France

[d] Dr. D. Hamdane
Institut de Biologie Paris-Seine, Biology of Aging and Adaptation, UMR 8256, Sorbonne Université 7 quai Saint-Bernard, 75 252 Paris, France

Supporting information for this article is available on the WWW under https://doi.org/10.1002/cbic.202300738

sequence similarity with Arh1p (and 36% sequence identity), was shown to reduce Yah1p efficiently,[6] and here proved functional in the adrenodoxin reductase/ferredoxin/Coq6p electron transfer system.

hAdxR, also known as ferredoxin reductase FdxR, is a mitochondrial FAD-dependent flavoenzyme belonging to the large and ubiquitous family of ferredoxin-NAD(P)$^+$ reductase (FNR). FNRs shuttle electrons between two-electron and one-electron carriers[7] and participate to many metabolic pathways such as steroid metabolism,[8] photosynthesis,[9] isoprenoid synthesis,[10] iron-sulfur cluster biogenesis.[11] The FNR family is organized into three phylogenetically and structurally unrelated protein groups, including the plastid-type, the thioredoxin reductase (TdR)-type and the glutathione reductase (GR)-type to which AdxR belongs to.

It has been shown that *adxR* is a p53 pro-apoptotic target gene that would sensitize cells to oxidative stress-induced apoptosis.[12] A hypothesis is that p53 would induce expression of AdxR, which would subsequently cause a depletion of the available pool of reduced NADPH necessary for detoxifying reactive oxygen species (ROS) in mitochondria, amplifying the ROS-mediated apoptosis. Indeed, an *adxR*-deficient mouse leads to embryonic lethality potentially due to iron overload. AdxR and p53 would be mutually regulated. This AdxR-p53 loop would play an important role in iron homoeostasis for tumor suppression.[13] Furthermore, a recent study has identified at least three mutations in the *adxR* gene (L215 V, R306 C and E477 K, Figure S1) of patients suffering from sensorial neuronal defects (auditory neuropathy and optic atrophy) and leading to mitochondrial iron overload.[14]

Human AdxR receives two electrons in the form of a hydride ion from NADPH and transfers them one at a time to [2Fe-2S] adrenodoxin (Adx, also called ferredoxin 1 or Fdx1), which then transports them to mitochondrial cytochrome P450 s.[15] In adrenal glands, these P450s are involved in the biosynthesis of steroid hormones (reviewed in).[8,16] In liver and kidney mitochondria, this electron transfer chain donates electrons to the cytochromes P450 involved in the production of bile acids and in the activation of vitamin D_3.[17] In addition to its important role in P450s metabolism, AdxR is involved in iron homeostasis,[18] *de novo* Fe–S cluster biogenesis[6,11a,19] and also heme O and heme A formation *via* ferredoxin 2 (Fdx2).[20] Human Fdx1 and Fdx2 share 43% sequence identity and a very similar structure. They both interact with the same NADPH dependent reductase, adrenodoxin reductase. While the classical function of Fdx1 is sterol synthesis via cytochrome P450 enzymes and the main function of Fdx2 is Fe/S cluster biogenesis and heme A synthesis,[6,20c] other studies have shown that both Fdx1 and Fdx2 would be important in iron/sulfur cluster synthesis. In particular, knock-down of Fdx1 would significantly compromise iron-sulfur proteins activities and would lead to mitochondrial iron overload.[19b] Moreover, recent studies have shown that Fdx1 is essential for production of the lipoic cofactor synthesized by the Fe-S lipoyl synthase.[21] Fdx1 is also required for the mitochondrial reduction and delivery of copper to Cytochrome c oxidase (CcO).[22] Most of the biochemical and structural studies were done on the native AdxR from *B. taurus* (bAdxR) purified from the adrenal cortex in the 1970 s,[23] and then on a recombinant version overexpressed and purified from *E. coli*.[24] This 54-kDa monomeric flavoprotein is loosely associated with the inner mitochondrial membrane[25] and contains one molecule of flavin adenine dinucleotide (FAD) per polypeptide chain.[23c] The crystal structure of bAdxR showed that the enzyme is organized into two domains, a FAD-binding domain and a NADP-binding domain of about equal size, with the active site lying at the interface of both domains. Furthermore, the structures of the protein in complex with dinucleotides revealed that the C4 of the nicotinamide moiety and the N5 of FAD are placed in a proper orientation for hydride transfer.[26] The structure of bAdxR-Adx complex revealed a slight reorientation of bAdxR domains, resulting in a shortening of the distance between the FAD and NADP domains.[27] In this complex, the distance between the FAD isoalloxazine ring of AdxR and the [2Fe-2S] cluster of Adx is 10.3 Å, which could support electron tunneling between the two redox centers. Bovine AdxR can be reduced not only by NADPH, but also by NADH, but the K_m value for NADPH (1.8 μM) is three orders of magnitude smaller than that for NADH (5 mM), suggesting that NADPH is the physiological electron donor for AdxR.[23c] It was proposed that this higher selectivity for NADPH over NADH was due to interactions between the 2′-phosphate group of NADPH and arginine residues in the nicotinamide binding domain.[28] This selectivity seems to be present in another protein of the AdxR family, FprA from *Mycobacterium tuberculosis*. FprA shares 39% and 40% sequence identity with bovine and hAdxR respectively, and is able to transfer electrons to the cytochromes P450 of *M. tuberculosis*.[29] It was found to be selective for NADPH.[29–30] A switch of selectivity of FprA towards NADH was observed when Arg200, the arginine responsible for interactions with the 2′ phosphate of NADPH, was mutated into alanine.[31] Although human and bovine AdxR share 88% sequence identity, the human counterpart has been much less studied than its bovine ortholog, probably due to the low-yield of protein expression in *E. coli* (0.1 mg/l culture).[32] Here, we report a protocol leading to a higher yield of expression of soluble recombinant hAdxR in *E. coli* allowing us to characterize in detail the reductive half-reaction between hAdxR and NAD(P)H by steady-state and transient kinetics using stopped-flow techniques. We showed that while the reaction of hAdxR with NADH obeys to a simple kinetic model, the enzymatic mechanism is far more complex with NADPH, due to reversible reactions likely driven by the great affinity of the enzyme for this reduced pyridine nucleotide. The weakening of this interaction by relatively low concentrations of $MgCl_2$, which acts as a competitive inhibitor with respect to NADPH binding, simplifies the mechanism rendering it amenable to a thorough kinetic investigation. We anticipate that such an approach could be implemented to study other related flavoenzymes sharing a similar complex reductive half-reaction with NADPH. The Alphafold2 model structure of hAdxR (Figure S1) show two arginine residues, R228 and R229, corresponding to R199 and R200 of FprA, which are very close to the 2′Phosphate groups of NADPH (Code PDB:1LQU).

Finally, we also establish *in vitro* the existence of a functional electron transfer chain from NADPH to the yeast monooxygenase Coq6p, via the flavin reductase AdxR and the [2Fe-2S] ferredoxin Yah1p. The discovery that AdxR and Yah1p mediate electron transfer from NADPH to Coq6p is unexpected because flavin monooxygenases are known to use NADPH or NADH as direct electron donors to their flavin cofactor.[5a,c] This novel scenario for reduction of flavoenzymes is discussed.

Results and Discussion

Expression, Purification and Spectroscopic characterization of hAdxR

In previous studies, human *adxR* gene was expressed in *E. coli* cells, using a derived-pFXblue plasmid with a bacteriophage λpL promoter, but gave a low yield of protein expression (~0.1 mg/liter of culture) due to the formation of inclusion bodies.[32] Here, the N-terminal hexahistidine (His_6)-tagged mature form of hAdxR, lacking the 32 N-terminal amino acids corresponding to the mitochondrial targeting sequence, was overexpressed in *E. coli* by using pETDuet-1 plasmid (Figure S2). The combination of (i) late protein induction (end of the exponential growth phase, $OD_{600nm} = 1.8$) with 0.2 mM IPTG, (ii) use of low temperature cultivation (20 °C for 18 hours) and (iii) co-expression of *E. coli* chaperones (GroES/GroEL), allowed us to increase the yield of soluble recombinant hAdxR by 25-fold (2.5 mg/L culture) compared to the previous protocols from literature. After the two steps purification, SDS-PAGE showed a main-band corresponding to a protein of ~50 kDa (Figure S3A) and SEC-MALS analysis showed that hAdxR behaves as a monomer in solution (Figure S3B). HPLC analysis of the flavin released from a heated hAdxR sample revealed that the enzyme binds FAD in a non-covalent manner. The visible absorption spectrum of hAdxR exhibits features typical of oxidized flavin-containing enzymes, with peaks at 271 nm, 376 nm and 450 nm, and shoulders at 420 and 478 nm (Figure S3C). The protein/flavin absorbance ratio at A_{271}/A_{450} nm is ~8. This spectrum is very similar to that of bAdxR[24a] or rat AdxR.[33] Based on an extinction coefficient of protein-bound FAD at 450 nm, $\varepsilon_{450} = 11\ mM^{-1}.cm^{-1}$, the FAD content of this hAdxR sample is ~0.7.

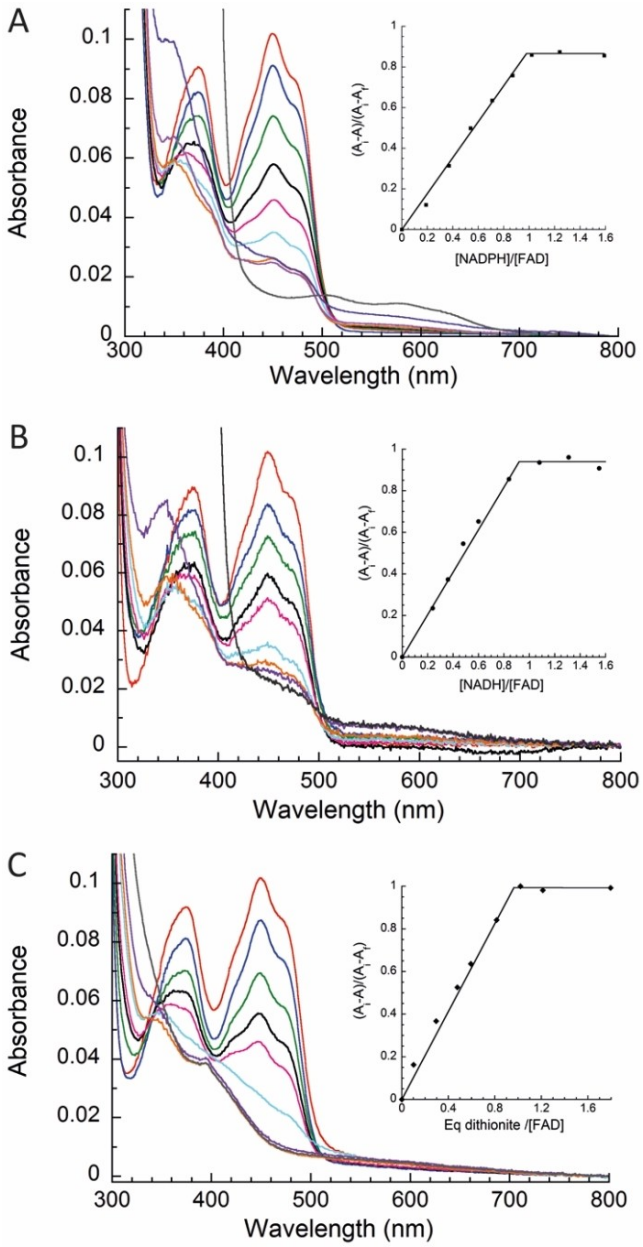

Figure 1. Redox titration of hAdxR with NADPH, NADH and dithionite. 9.3 μM hAdxR was stepwise reduced in anaerobiosis by NADPH (A) or NADH (B) or dithionite (C), in a 10 mm path length cuvette, in 100 mM Tris-HCl, pH 7.5. The last curve in (A) and (B) correspond to a molar ratio NADPH/FAD and NADH/FAD of 100:1. The insets show the plot of the fractional absorbance changes at 450 nm as a function of reductant/FAD molar ratio. A_i and A_f are the initial and final values of absorbance at 450 nm, respectively.

Reductive titration of hAdxR

The titrations of hAdxR by NADPH, NADH or dithionite were performed under anaerobic conditions to characterize the reactivity of the FAD coenzyme (Figure 1). Figure 1A shows the spectral changes of hAdxR in the presence of increasing amounts of NADPH. Upon addition of sub-stoichiometric amounts of NADPH, we observed that absorbance at 450 nm and 376 nm decreased steadily, which is consistent with the reduction of FAD into $FADH_2$. Concomitant to this decrease, we observed the appearance of a small and broad band between 500 and 700 nm, usually ascribed to the formation of a blue neutral FAD semiquinone, as this is the case for FprA.[30] When stoichiometry was reached, 85% of FAD was reduced but 15% remained oxidized, indicating an incomplete reduction, as this is observed in the case of bovine AdxR.[34] Similar results were observed when NADH was used as a reducing agent (Figure 1B). However, when titration was conducted with one equivalent dithionite, a full reduction of hAdxR was achieved, notably without formation of charge transfer bands (Figure 1C). This incomplete reduction by stoichiometric amounts of NAD(P)H is

not uncommon within the AdxR family, as examplified by the case of bAdxR,[34] and FprA from *M. tuberculosis*.[29–30]

Steady-state enzyme activities of hAdxR

To investigate whether hAdxR can discriminate between NADPH and NADH, we measured the ferricyanide reduction activity under steady-state conditions (Table 1). The reduction of ferricyanide proceeds with similar catalytic rate constants for both NADPH and NADH, k_{cat} (~26 s^{-1}). This rate is likely attributable to the limiting hydride transfer suggesting that the hydride is transferred at a similar rate from the nicotinamide moiety of NADPH or NADH. However, the apparent K_m for NADPH (2.6 ± 0.4 μM) is 65-fold lower than that for NADH (170 ± 13 μM), showing that hAdxR has a better affinity for NADPH. This translates into a higher catalytic efficiency with NADPH ($k_{cat}/K_m = 9.8 \pm 1.1\ \mu M^{-1}.s^{-1}$ for NADPH vs 0.15 ± 0.01 $\mu M^{-1}.s^{-1}$ for NADH). Overall, our results indicate that NADPH is a more effective reducing agent than NADH for hAdxR. This selectivity seems to be a general feature among the ferredoxin-reductase type enzymes.[35] Moreover, the estimated NADH/NADPH ratio in the mitochondrial matrix is estimated to be 1 over 1000, reinforcing our finding.[36]

30 nM hAdxR was incubated with various amounts of NADPH (1 to 100 μM) or NADH (10 to 2000 μM) in the presence of 1 mM ferricyanide, in a total volume of 500 μl, in buffer Tris-HCl 100 mM, pH 7.5. The ferricyanide concentration was kept at 1 mM when measuring the K_m for NADPH, and at 200 μM when measuring the K_m for NADPH. When measuring the K_m for ferricyanide, 100 μM of NADPH or 1500 μM of NADH were used. *nd*, not determined.

The apparent discrepancy between the K_m values of hAdxR for ferricyanide, which are 10 times lower when using NADH than NADPH, could possibly be explained by a competitive interaction between $NADP^+$ and ferricyanide for binding to the reduced hAdxR (see stopped flow), which may not be the case with NAD^+.

Stopped-flow kinetics of hAdxR anaerobic reduction with NADH

The kinetics of anaerobic reduction of hAdxR by NADH were studied with a stopped-flow spectrophotometer in a single-wavelength mode at 25 °C. The flavin reduction was monitored by recording the absorbance change at 450 nm over time after the rapid mixing of 800 μM NADH with 15 μM hAdxR in a phosphate buffer. As shown in Figure 2A, the variation of absorbance within 200 ms of reaction accounts for conversion of oxidized FAD into $FADH_2$. The FAD reduction was fitted to a single exponential function yielding an apparent rate constant of ~24 ± 0.2 s^{-1}, a value similar to the k_{cat} (26 ± 0.5 s^{-1}) for the steady-state reduction of ferricyanide by NADH (Table 1). In contrast, the kinetic followed at 530 nm is biphasic with a rapid increase of absorbance during the first ~18 ms followed by subsequent decrease (Figure 2A). The first kinetic phase is attributed to the formation of charge transfer 1 (CT1), which generally corresponds to the Michaelis complex (i.e AdxR-FAD·NADH), while the second phase represents the decay of CT1 concomitant to the hydride transfer reaction. The formation of this complex proceeds with a k_{obs1} of ~92.5 ± 3 s^{-1} while it disappears at 26 ± 1.5 s^{-1} consistent with the apparent rate constant for FAD reduction determined at 450 nm (AdxR-FAD + NADH,$H^+ \rightarrow$AdxR-FAD·NADH,$H^+ \rightarrow$AdxR-$FADH_2$ + NAD^+). It was not possible to observe any detectable signal at 700 nm for the charge transfer 2 (CT2) attributed to the AdxR-$FADH_2$·NAD^+ species, which is in agreement with a fast dissociation of NAD^+ product from the reduced enzyme. Accordingly, the hydride transfer from the nicotinamide to FAD is likely the rate-limiting step in the reaction of hAdxR with NADH.

The reductive half-reaction of hAdxR was further examined over a wide range of NADH (0.025 to 1.6 mM) (Figure 2B). All the kinetics traces monitored at 450 and 530 nm were treated with a single and double exponential function, respectively. The observed rate constants for FAD reduction exhibits a hyperbolic dependence on NADH concentration reaching a plateau ~29 s^{-1} (k_{lim}) and intercepting the *y*-axis around zero, which is consistent with an essentially irreversible reduction step of FAD. The rate constants of CT1 formation vary linearly with NADH concentration yielding a slope of 0.075 ± 0.01 $\mu M^{-1}.s^{-1}$ and a *y*-intercept C of 37 ± 3 s^{-1}. On the basis of k_{obs} dependency on NADH for both the CT1 formation and flavin reduction, microscopic rate constants that account for the minimal model illustrated by Scheme 1 can be estimated. The bimolecular rate constant k_1 is 0.075 ± 0.01 $\mu M^{-1}.s^{-1}$ while the k_{-1} can be calculated from $C = k_{lim} + k_{-1}$ yielding a value ~8 s^{-1}. The k_{lim} value is assigned to the k_2~29 s^{-1}. The dissociation constant K_d for NADH is thus k_{-1}/k_1~107 μM.

Table 1. Steady-state activity of hAdxR assessed by ferricyanide reduction.

Electron Acceptor Ferricyanide								
	No $MgCl_2$				25 mM $MgCl_2$		100 mM $MgCl_2$	
	K_m NAD(P)H (μM)	K_m ferricyanide (μM)	k_{cat} (s^{-1})	k_{cat}/K_m ($\mu M.s^{-1}$)	K_m NAD(P)H (μM)	k_{cat} (s^{-1})	K_m NAD(P)H (μM)	k_{cat} (s^{-1})
NADPH	2.6 ± 0.4	131 ± 16	25.6 ± 0.7	9.8 ± 1.1	8 ± 0.9	30 ± 3	26.5 ± 1.8	42 ± 2
NADH	170 ± 13	12.8 ± 0.7	26 ± 0.5	0.15 ± 0.02	*nd*	*nd*	*nd*	*nd*

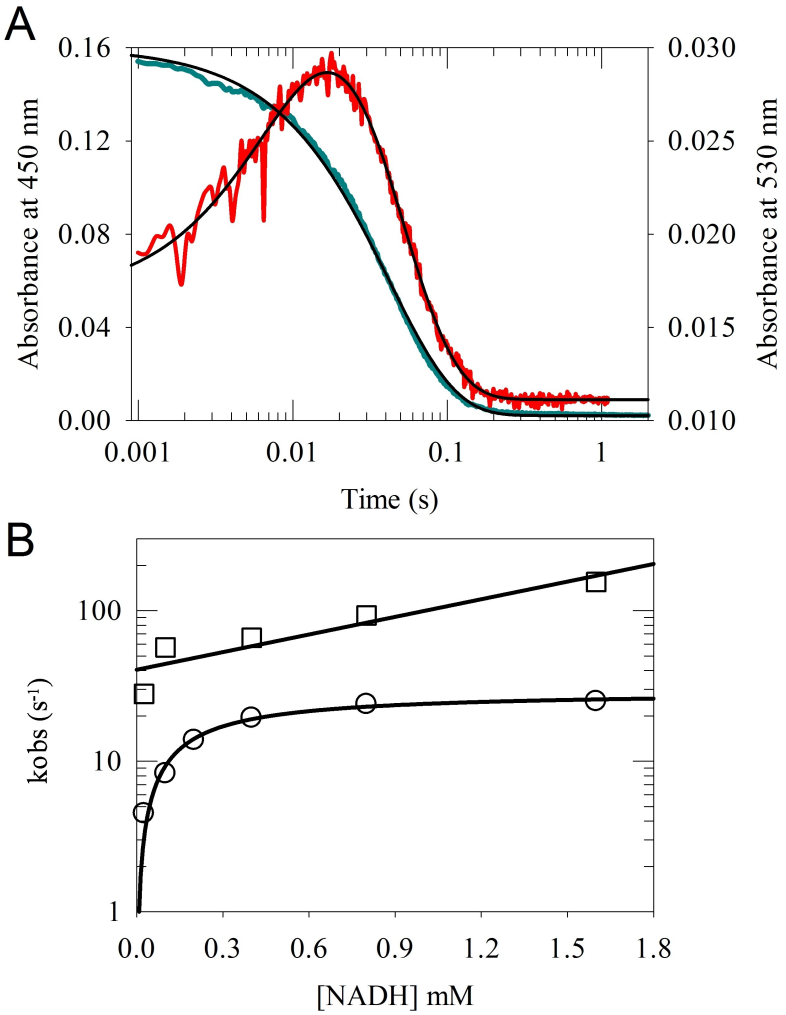

Figure 2. Kinetics of reduction of hAdxR by NADH. (A) Kinetic traces of hAdxR (15 μM) reduction by NADH recorded by following the absorbance at 450 (left axis, green) and 530 nm (right axis, red). (B) Dependence of the observed rate constant for hAdxR reduction (k_{obs}) as a function of NADH determined at 450 nm (circle) and 530 nm (square).

The enzyme first binds NADH forming a Michaelis complex at 92.5 s^{-1}, a rate attributed to the charge transfer 1 formation. Then, the flavin reduction occurs at a rate of 26 s^{-1} (k_{lim}), consistent with the k_{cat} value determined from ferricyanide reductase activity and reflecting the rate-limiting step in the reaction cycle. This apparent first order rate constant varies hyperbolically with NADH, in accordance with the minimal model in Scheme 1 with a quasi-irreversible hydride transfer as evidenced from the absence of a detectable signal for NAD^+/$FADH^-$ charge transfer CT2 complex and the hyperbolic dependence intercepting the y-axis near zero leading to a K_d for NADH~107 μM.

Stopped-flow kinetics of hAdxR anaerobic reduction by NADPH

The reduction of hAdxR was also studied with NADPH. Rapid mixing of 12.5 μM hAdxR with 64 molar equivalents of NADPH led to a loss of absorbance at 450 and 530 nm (Figure 3A).

The variation of absorbance at 450 nm indicates that all the FAD of hAdxR is reduced within 200 ms. Both kinetic traces were best fitted with a monophasic exponential yielding comparable observed rate constants 27 ± 0.5 s^{-1} and 29 ± 0.8 s^{-1} at 450 and 530 nm, respectively (Figure 3A). These rate constants are similar to those observed for the reduction of hAdxR by NADH suggesting that the hydride transfer step from

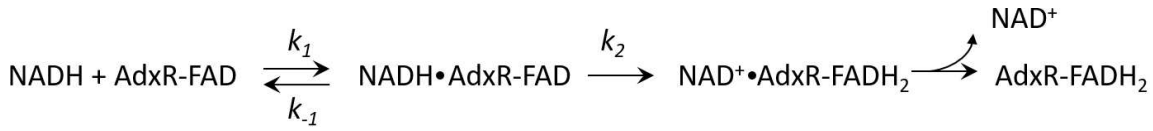

Scheme 1. Minimal model for the reaction of hAdxR with NADH.

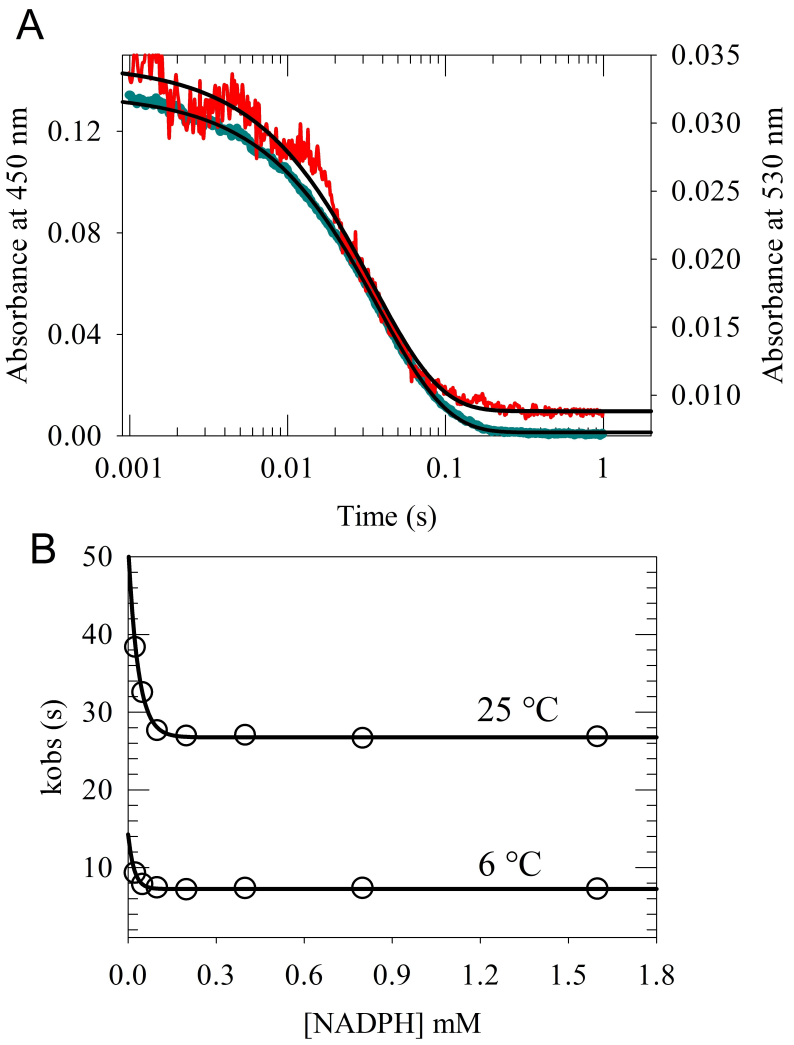

Figure 3. Stopped-flow kinetics of reduction of hAdxR by NADPH. (A) Kinetic traces of hAdxR (12.5 μM) reduction by 64-molar equivalent of NADPH recorded by following the absorbance at 450 (left axis, green) and 530 nm (right axis, red). (B) Dependence of the observed rate constant for hAdxR reduction (k_{obs}) as a function of NADPH determined at 450 nm at 25 °C or 6 °C.

the nicotinamide to FAD occurs at a similar rate with NADH or NADPH. A notable difference with NADH is the lack of detectable kinetic phase attributed to the AdxR-FAD·NADPH complex formation (Figure 3A), even at lower temperature (T = 6 °C) (Figure 3B). The kinetics of AdxR reduction were also recorded with various concentration of NADPH at 25 °C. As shown in Figure 3B, the observed rate constant for flavin reduction observed at either 450 or 530 nm does not exhibit a classical rectangular hyperbolic dependence on NADPH but rather it decreases with increasing NADPH concentration from 38.5 ± 0.5 s^{-1} at 25 μM to a limiting value of 27 ± 0.3 s^{-1} (k_{lim}) at saturating NADPH, the latter value consistent with the rate of hydride transfer. This kinetic behavior was conserved even at low temperature (Figure 3B) preventing us from determining the microscopic constants for the reaction of NADPH with the enzyme. In fact, this phenomenon has also been observed in other flavoenzymes such as the members of CYPOR family (cytochrome-P450 reductase, NO synthase, flavocytochrome P450-BM3 reductase)[37] and FprA from *M. tuberculosis*[30] but not in the case of canonical FNRs.

The failure to fit the FAD reduction rate constants versus the NADPH concentration to a simple Michaelis type equation might be due to: (i) a reversible hydride transfer combined with a high affinity of the reduced enzyme for the $NADP^+$ product and (ii) a possible binding of $NADP^+$ to the oxidized enzyme.[37c] To verify if $NADP^+$ could oxidize $FADH_2$ of hAdxR, the enzyme was reduced with a stoichiometric amount of NADPH and rapidly mixed with a large excess of $NADP^+$. This resulted in an increase of absorbance at 450 nm consistent with a $FADH_2$ oxidation by $NADP^+$ proceeding at 46 s^{-1} (Figure S4). This reversible hydride transfer in AdxR family is likely to occur because of the high affinity of the hAdxR for NADPH and $NADP^+$ much larger than that for NADH/NAD^+.

Effect of Mg^{2+} on the steady state kinetics

Mg^{2+} is a physiological cation often involved in the interaction with the negatively charged phosphates of single or polynucleotides such as RNA.[38] It acts as a cofactor of several important enzymes requiring Mg–ATP complex for full functionality, such as various protein kinases, proteins involved in nucleic acid metabolism, or ATPases involved in the transport of various ions. Furthermore, Mg^{2+} binds to phosphate groups present in nucleic acid polymers. Since NAD(P)H carries phosphates, we wondered if Mg^{2+} could influence the catalytic properties of hAdxR. Therefore, the rate of ferricyanide reduction using NADPH as the electron source was measured in the presence of various concentrations of $MgCl_2$ (Table 1). Increasing $MgCl_2$ from 0 to 25 mM resulted in a 3-fold increase of the K_m for NADPH while the k_{cat} remained almost unchanged. As the concentration of $MgCl_2$ increased, this effect became more pronounced, with a 10 and 1.6-fold increase at 100 mM $MgCl_2$ for the K_m and k_{cat} as compared with those determined in the absence of $MgCl_2$, respectively. The resulting 6-fold decrease in catalytic efficiency (k_{cat}/K_m) is mainly due to a lower affinity of the enzyme for NADPH. The role of Mg^{2+} is reminiscent of that of a competitive inhibitor as indicated by the plot of the apparent K_m for NADPH versus $MgCl_2$, yielding a Ki value of ~4.5 mM (Figure S5).

Effect of $MgCl_2$ on the anaerobic NADPH reduction of hAdxR under pre-steady-state conditions

To further decipher the impact of Mg^{2+} on hAdxR activity, the anaerobic NADPH reduction kinetics of hAdxR were measured by stopped-flow spectrophotometry with various $MgCl_2$ concentrations. Because, Mg^{2+} can react with phosphate buffer and form precipitates, Tris buffer was chosen as the working buffer. In the absence of Mg^{2+}, the kinetics recorded at 450 nm and 530 nm were identical to those measured in the presence of phosphate, allowing us to determine the exact contribution of Mg^{2+} on the kinetics mechanism of hAdxR (Figure 4).

In the presence of 25 mM $MgCl_2$, the evolution of the observed rate constants for FAD reduction changes completely as the trace regains a hyperbolic function. However, fitting the data to this classical function $k_{obs} = k_{lim}x[NADPH]/(K_d + [NADPH])$ is still not possible. Indeed, the reciprocal plot of $1/k_{obs}$ versus 1/[NADPH] is markedly nonlinear except at high NADPH concentration indicating that the reverse hydride transfer step ($FADH_2 + NADP+ \rightarrow FAD + NADPH$) proceeds with a finite rate constant, k_{-2}. The situation became simpler at 50 mM and 100 mM $MgCl_2$ as the k_{obs} for flavin reduction *vs* [NADPH] evolved according to a perfect rectangular hyperbolic function enabling a more accurate determination of the K_d for NADPH and a microscopic constant for the flavin reduction. This is confirmed by the double reciprocal plot ($1/k_{obs}$ vs 1/[NADPH]) which yielded a straightline plot consistent with the rapid binding equilibrium between NADPH and hAdxR, and consequently a negligible rate constant for the reverse hydride transfer reaction. The K_d for NADPH were 10 μM and 33.5 μM and the k_2 values were ~32 s^{-1} and 34 s^{-1} in the presence of 50 mM and 100 mM $MgCl_2$ respectively.

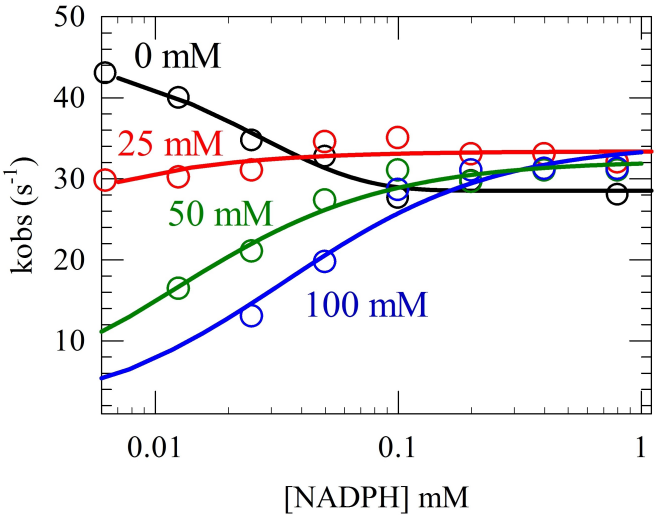

Figure 4. Effect of $MgCl_2$ on the kinetics of reduction of hAdxR with NADPH. Dependence of the observed rate constant for hAdxR reduction (k_{obs}) as a function of NADPH determined at 450 nm in the presence of different $MgCl_2$ concentrations as indicated on each curve.

Here we were able to obtain a classical Michaelis-Menten behaving enzyme with NADPH by using low concentration of $MgCl_2$ ($\leq$100 mM) at physiological pH 7.5. Interestingly, Pennati et al., showed that, by using very high NaCl concentration (2.5 M) combined with a high pH of 10, FprA from *M. tuberculosis* also has a lower affinity for NADPH.[39] Thus, we obtained a similar result but in much milder physiological conditions. In another approach, Sabri et al showed that mutation of Arg199 and Arg200 in FprA, two residues interacting with the NADPH 2′-phosphate group, decreased the affinity for NADPH, abolished electron transfer from FAD hydroquinone to $NADP^+$ and allowed to recover a hyperbolic dependence of NADPH-dependent FAD reduction.[31]

Detection of the AdxR-FAD·NADPH complex in the presence of $MgCl_2$

In the absence of $MgCl_2$, it was not possible to observe the transient formation of AdxR-FAD·NADPH species. Thus, lowering the affinity of the enzyme for NADPH may render accessible the detection of the complex formation. For that purpose, the anaerobic kinetics of hAdxR flavin reduction with NADPH were performed at 50 and 100 mM $MgCl_2$ and followed at 530 nm (Figure 5).

At 50 mM $MgCl_2$, after mixing oxidized hAdxR with a molar equivalent of NADPH, a fast increase of absorbance at 530 nm was observed within the first 13 ms, with an observed rate constant of 15.2 s^{-1}. This phase was followed by a loss of absorbance at ~22 s^{-1}, which is similar to that determined at 450 nm under the same experimental conditions. Increasing NADPH concentration resulted in an acceleration of the rates of AdxR-FAD·NADPH formation (Figure 5 inset). At >0.2 mM of

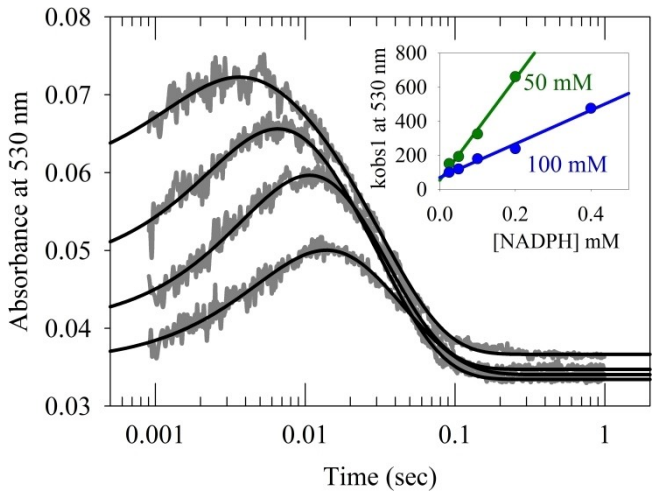

Figure 5. Effect of $MgCl_2$ on the transient formation of AdxR-FAD·NADPH complex. Kinetic traces of hAdxR reduction (25 μM) by NADPH in the presence of various $MgCl_2$ concentration (25, 50, 100 and 200 mM $MgCl_2$) recorded by following the absorbance at 530 nm. The inset shows the linear dependence of the observed rate constant for AdxR-FAD·NADPH formation with respect to NADPH concentration determined in the presence of 50 mM or 100 mM $MgCl_2$.

NADPH, the formation of this intermediate became hardly detectable occurring within less than 1 ms. At 100 mM $MgCl_2$, the stability of the AdxR-FAD·NADPH was increased as the CT1 signal remained observable at concentrations of NADPH up to 0.4 mM. The observed rate constant for the CT1 formation (k_{obs1}) is linearly dependent on NADPH concentration consistent with the minimal simple reversible equilibrium as shown in the Scheme 2:

Accordingly, the slope representing the k_1 yielded a value of ~2.9×10^3 $mM^{-1}.s^{-1}$ and ~0.9×10^3 $mM^{-1}.s^{-1}$ for 50 and 100 mM $MgCl_2$, respectively. Because the *y*-intercepts of k_{obs} at both $MgCl_2$ concentrations *vs* NADPH concentration were not significantly different, the increase of K_d for NADPH provoked by $MgCl_2$ was mainly due to a decrease of k_1.

Altogether these results show that $MgCl_2$ does not affect the hydride transfer rate and it would exert its role by impairing NADPH binding through interaction with its ADP moiety. Indeed, $MgCl_2$ lowers the K_d for NADPH enabling us to detect for the first time in mammalian AdxR the formation of a Michaelis complex between the oxidized enzyme and NADPH at an observed rate of ~15 s^{-1} in the presence of 50 mM $MgCl_2$, and its subsequent consumption by the hydride transfer step.

To test if the effect of $MgCl_2$ was specific to NADPH, the kinetics of flavin reduction by NADH in the presence of $MgCl_2$ was also measured. Like in the case of NADPH, $MgCl_2$ seemed to affect the K_d of hAdxR for NADH without impairing the rate

$$\text{NADPH + AdxR-FAD} \underset{k_{-1}}{\overset{k_1}{\rightleftharpoons}} \text{NADPH•AdxR-FAD}$$

Scheme 2. Michaelis-Menten complex formation of NADPH with hAdxR.

of the hydride transfer. Going from 0 to 50 mM $MgCl_2$ resulted in ~6-fold increase of the K_d for NADH (from 170 μM at 0 mM to ~1 mM at 50 mM $MgCl_2$) (Figure 6).

It is important to note that although a concentration of 25 mM or higher of Mg^{2+} is required to modify the kinetic behavior of hAdxR, this concentration is well above the concentration of free Mg^{2+} in the cell (0.8–1.2 mM).[40] However, it should be taken into consideration that most of the total amount of Mg^{2+} (15–200 mM)[41] is in a bound form, mainly to proteins, nucleic acids, and nucleotides. Therefore, it is conceivable that hAdxR binds to the NADPH complex chelated by Mg^{2+}, promoting a Michaelian mechanism for the enzyme *in vivo*.

Expression, purification and characterization of Coq6p and Yah1p from Saccharomyces cerevisiae

Then, with functional hAdxR at hand, we turned to investigating the reason for the requirement of Arh1p and Yah1p for the activity of the monooxygenase Coq6p involved in a hydroxylation step of the coenzyme Q biosynthesis pathway, as established by *in vivo* experiments in *S. cerevisiae*.[4] Despite Coq6p belonging to class A monooxygenases, we hypothesized that FAD reduction in Coq6p may not occur via direct reduction by NADPH but instead via indirect reduction by NADPH using the Arh1p/Yah1p electron transfer system. In order to test this hypothesis, we first expressed and purified the Coq6p and Yah1p recombinant proteins from *S. cerevisiae*, and then used hAdxR instead of its yeast homolog Arh1p, since we could not obtain this protein despite numerous attempts.

We previously reported the expression and purification of yeast Coq6p, as an MBP-tag fusion protein. The purified tetrameric Coq6p-MBP is a flavoprotein with 0.85 FAD/monomer. However, cleavage of the MBP tag resulted in aggregation that prevented any biochemical study.[3b] To overcome this

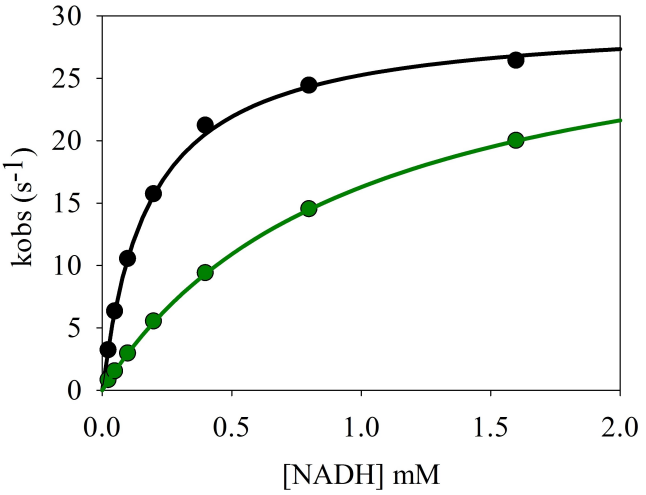

Figure 6. Effect of $MgCl_2$ on the kinetics of reduction of hAdxR with NADH. Dependence of the observed rate constant for hAdxR reduction (k_{obs}) (25 μM) as a function of NADH determined at 450 nm in the absence of $MgCl_2$ (green curve) or in the presence of 50 mM $MgCl_2$ (black curve).

problem, we decided to remove the 24 N-terminal amino acids corresponding to the mitochondrial targeting sequence and overexpressed and purified this mature form of Coq6p as a MBP-tag fusion protein (Figure S6). Coq6pΔ1-24-MBP was purified using two chromatographic steps: (i) an affinity MBP-trap and (ii) a Superdex 200 gel filtration. After removal of the MBP tag by Factor Xa, Coq6pΔ1-24, hereafter called mature Coq6p showed a prominent band at ~50 kDa on SDS-PAGE (Figure S7A) and behaved as a monomer of 48 kDa, as shown by SEC-MALS analysis (Figure S7B). Overall, 2 mg of mature Coq6p could be obtained from 1 L of culture medium. The visible absorption spectrum of mature Coq6p exhibits features typical of flavin-containing enzymes, with peaks located at 275 nm, 382 nm and 449 nm, and shoulders at 420 and 478 nm. The protein/flavin absorbance ratio at A_{275}/A_{449} nm in the oxidized form of the enzyme is 10.1 (Figure S7C). The molar extinction coefficient of mature Coq6p is 11.5 $mM^{-1}.cm^{-1}$ at 449 nm and this enzyme presents a stoichiometry of 0.85 mole FAD per mole of monomer.

Expression of yeast Yah1pΔ1-57 lacking the mitochondrial targeting sequence (Figure S8) led to a large production of soluble recombinant protein. As the protein does not bear any tag, it was purified with two chromatographic steps. After an anion exchange column (UnoQ6) and a gel filtration step (Superdex 75), the protein was found to be pure to homogeneity, as judged by SDS-PAGE (Figure S9A). Overall, 25 mg of Yah1pΔ1-57 could be obtained from 1 L of culture medium. Mature Yah1p is a monomer of 13 kDa, as judged by gel filtration (Figure S9B). Quantitation of iron (1.7 ± 0.2 per protein) and sulfur (2.1 ± 0.2 per protein) were in good agreement with the expected presence of one [2Fe-2S] cluster within a single polypeptide chain. The UV-visible absorption spectrum of mature Yah1p exhibits bands at 341 nm, 414 and 457 nm, which are characteristics of an oxidized $[2Fe\text{-}2S]^{2+}$ cluster (Figure S9C). The absorbance ratio at A_{280}/A_{414} nm in the oxidized form of the enzyme is 1.8. The molar extinction coefficient calculated are 14.5 $mM^{-1}cm^{-1}$ at 341 nm, 11 $mM^{-1}cm^{-1}$ at 414 nm and 9.3 $mM^{-1}cm^{-1}$ at 457 nm.

Therefore, we chose to replace Arh1p with hAdxR in the subsequent *in vitro* assays since these two proteins are homologous (36% sequence identity (Figure S10)) and hAdxR was shown to reduce Yah1p efficiently.[6]

Electron transfer chain from NADPH to Coq6p via AdxR and Yah1p

In class A flavin monooxygenases, the FAD cofactor is typically reduced by direct hydride transfer from NADPH, as a prerequisite for O_2 activation.[5c] The reduction of the FAD of mature Coq6p with a large excess (50-fold) of NADH or NADPH under anaerobic conditions was monitored by UV-visible spectroscopy. As shown in Figure 7A, no FAD reduction was observed after prolonged incubation of mature Coq6p with NADPH. Furthermore, Coq6p exhibited no NADH oxidase activity, consistent with the inability of NADH to reduce FAD. In contrast, the redox titration of Coq6p with dithionite showed a full reduction with one equivalent dithionite indicating that the FAD was redox reactive (Figure S7D). The effects of hAdxR alone or in combination with Yah1p on the anaerobic reduction of Coq6p by NADPH was studied spectrophotometrically as follows (Figure 7). Importantly, hAdxR was previously shown to reduce Yah1p efficiently *in vitro*.[6]

Addition of hAdxR to the Coq6p-NADPH mixture immediately resulted in a small increase of the absorption band at 450 nm and the appearance of the hAdxR-characteristic $FADH_2$-$NADP^+$ charge transfer band above 500 nm indicating reduction of FAD from hAdxR by NADPH (Figure 7A). No further modification occurred with time, in particular no decay of the absorption band at 450 nm, demonstrating that the NADPH-hAdxR system was not competent for reduction of FAD of Coq6p. (Figure 7A). Finally, when Yah1p was added to the NADPH/hAdxR/Coq6p mixture, the reduction of the FAD from Coq6p occurred instantaneously and was complete within a few minutes (Figure 7B). The reduction of Coq6p was biphasic with a fast phase, k_{obs1}~1.25 min^{-1}, accounting for 62% of the absorbance change at 450 nm, while the second phase was characterized by a k_{obs2}~0.1 min^{-1} (Figure S11). In order to demonstrate that Coq6p receives its electrons specifically from Yah1p, the latter was first reduced by a stoichiometric amount of dithionite. As shown in Figure S9D, the spectral variation following titration with dithionite indicated a complete reduction of the $[2Fe\text{-}2S]^{2+}$ center of Yah1p to a $[2Fe\text{-}2S]^{+}$ center (characterized by a band at 550 nm) with 1 equivalent of dithionite. The anaerobic addition of this reduced form of Yah1p to oxidized Coq6p resulted in the reoxidation of Yah1p as shown by the increase in absorbance at 508 nm (Figure 7C), a wavelength corresponding to an isosbestic point specifically for the reaction $FAD -> FADH_2$ (Figure 7B). The parallel reduction of Coq6p (Figure 7B) and oxidation of Yah1p (Figure 7C) clearly indicates an interprotein electron transfer from the $[2Fe\text{-}2S]^{+}$ of Yah1p to the FAD of Coq6p. The oxidation kinetics of Yah1p by Coq6p is biphasic, with a fast phase (~66%) exhibiting a k_{obs} of $2.5 +/- 0.1$ min^{-1} and a slow phase (~34%) with a k_{obs} of $0.3 +/- 0.08$ min^{-1}. Taken together, these results unambiguously demonstrate that (i) the FAD from Coq6p cannot be reduced by NAD(P)H; (ii) Coq6p is reduced by the NADPH/Arh1/Yah1p electron transfer chain; and (iii) Yah1p is the protein involved in the direct reduction of Coq6p (Figure 7D).

Remarkably, two other flavin monooxygenases were also suggested to be reduced by NADPH indirectly (Figure S12): (i) the pepper zeaxanthine epoxidase catalyzes epoxidation of zeaxanthin and is proposed to receive its reducing equivalents from the heterologous spinach ferredoxin reductase/ferredoxin system;[42] and (ii) human squalene monooxygenase catalyzes the monooxygenation of the triterpenoid squalene and is proposed to obtain electrons from NADPH-cytochrome P450 reductase.[43] Hence, our results with *S. cerevisiae* Coq6p establish a novel scenario of a flavin monooxygenase relying on specific reductases for the reduction of its FAD cofactor. We note that human Coq6 is unlikely to rely on a ferredoxin reductase/ferredoxin system since human FDX1 and FDX2 were shown recently to be dispensable for CoQ biosynthesis in human cells.[11b] Overall, it remains to be determined which

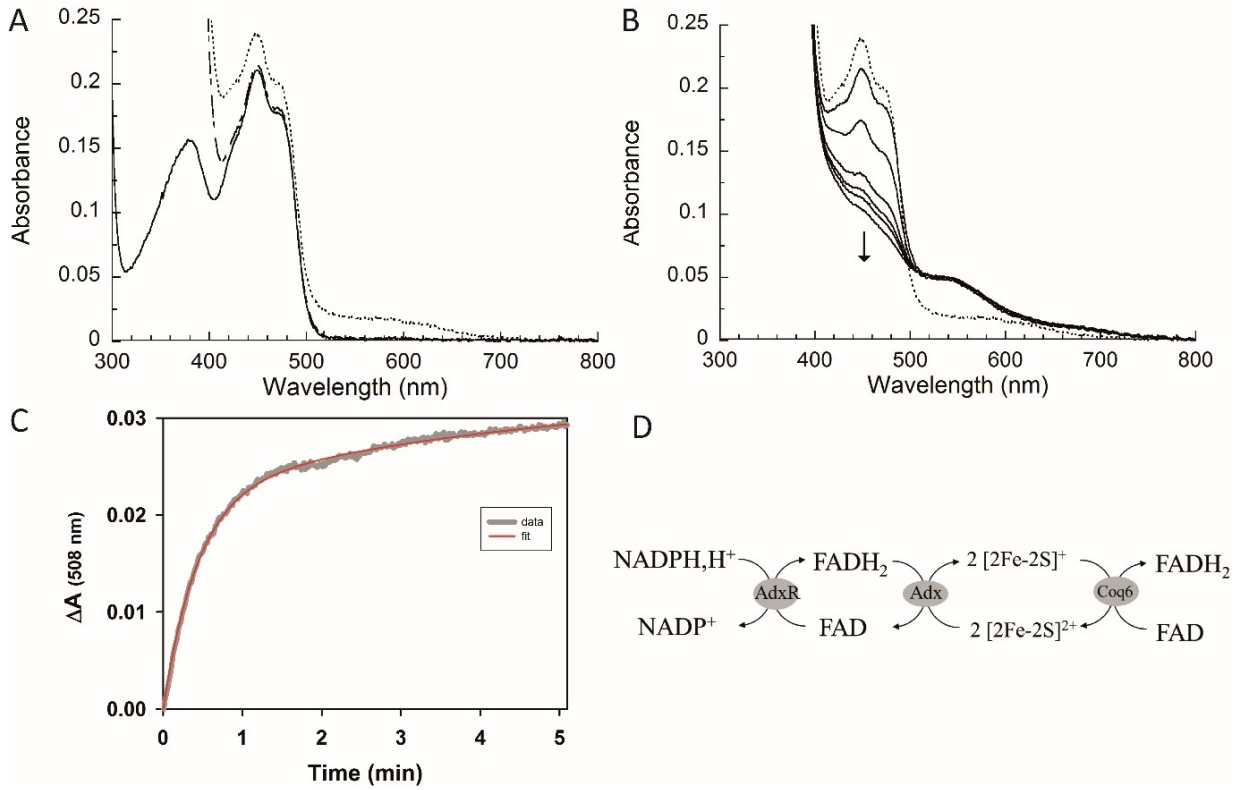

Figure 7. Evidence of an electron transfer chain, NADPH/hAdxR/Yah1p, for Coq6p reduction under anaerobic conditions. (A) UV-visible spectrum of Coq6p (18 μM) alone (solid line) or in the presence of 50-fold molar excess of NADPH (– – –), or in the presence of 50-fold molar excess of NADPH and hAdxR (10 μM) (dotted line). (B) Variation of the UV-visible spectrum of the mixture containing Coq6p (18 μM), NADPH (1 mM), hAdxR (10 μM) following the addition of Yah1p (10 μM). The spectra were recorded after 15 s, 30 s, 2 min, 3.5 min, 6.5 min and 9 min incubation time. The band at 550 nm is characteristic of reduced Yah1p (see Figure S9D). (C) Kinetics of reoxidation of dithionite-reduced Yah1p (50 μM) by mature Coq6p (10 μM) recorded at 508 nm. (D) Scheme of the electron transfer chain from NADPH to Coq6p via AdxR and Adx.

Coq6p homologs rely on a ferredoxin reductase/ferredoxin system and why some class A FAD monooxygenases evolved to use indirect systems to mediate the reducing power from NADPH to the flavin cofactor, rather than the classical direct hydride transfer.

Conclusions

In conclusion, by optimizing the yield of expression of the recombinant enzyme in *E. coli*, we have been able to perform stopped-flow kinetics allowing us to decipher the enzymatic reaction of human AdxR with its NAD(P)H substrate. We showed that like other related FAD-dependent flavoenzymes, the reaction with NADH obeys to a classical Michaelis-Menten behavior while that with NADPH is far more complex. Destabilizing the AdxR:NADPH complex with $MgCl_2$ proved to be a simple procedure to convert the enzyme into a classical behaving Michaelis-Menten flavoenzyme allowing us to explore in details the reductive half-reaction of human hAdxR with NADPH. This will certainly benefit future studies on the human AdxR-Adx reducing system and its redox partners. More broadly, we believe that the destabilization of NADPH binding by $MgCl_2$ could be helpful to study other flavoenzyme systems bearing a complex mechanism. In addition, we established via *in vitro* and spectroscopic studies that the Coq6p monooxygenase, involved in the biosynthesis of coenzyme Q, relies on the NADPH/AdxR/Adx electron transfer chain for its reduction.

Experimental Procedures

Strains and Plasmids

BL21 (DE3) *E. coli* strains were purchased from Novagen. Plasmid pGro7 encoding the chaperones GroES and GroEL under the control of the inducible *araB* promoter was purchased from TaKaRa Bio, Inc. (Japan). The pETDuet-1 plasmid (Novagen) containing the mature cDNA sequence of the hAdxR, lacking the 32 N-terminal aminoacids, cloned between *Eco*RI and *Not*I restriction sites, was kindly provided by U. Mühlenhoff.[20c] The pET15b plasmid for the overexpression of the mature sequence of Yah1p from *Saccharomyces cerevisiae*, lacking the 57 N-terminal aminoacids, was kindly provided by U. Mühlenhoff.[20c] The mature sequence of Coq6p from *Saccharomyces cerevisiae*, lacking the 24 N-terminal aminoacids was cloned into the pMAL-c2X plasmid (New England Biolabs) between *Bam*HI and *Hind*III restriction sites.

Expression and purification of human recombinant hAdxR

Overexpression of hAdxR was achieved by using BL21(DE3) *E. coli* strain co-transformed with pGro7/pETDuet-1-hAdxR and grown in

Luria-Bertani (LB) medium containing ampicillin (100 μg/ml) and chloramphenicol (34 μg/ml), shaking at 200 rpm and 37 °C. When A_{600nm} reached~1.8, arabinose was added to a final concentration of 2 mg/ml, the culture was cooled to 20 °C for 30 min, IPTG was added to a final concentration of 0.2 mM, and incubation at 20 °C was continued for 18 hours. The cells were harvested when A_{600nm} reached~5 and pelleted by centrifugation at 5000×*g* for 10 min. All subsequent operations were carried out at 4 °C. The cells (~36 g, wet weight) were resuspended in 6 volumes of buffer A (20 mM Tris-HCl, pH 7.5, 500 mM NaCl, 20 mM imidazole). Two tablets of cOmplete protease inhibitors cocktail (Roche) were added. Cells were lysed by sonication (Branson Digital Sonifier 450) with amplitude of 40% for 10 min with 30 s on/30 s off intervals, and subjected to ultracentrifugation at 180,000×*g* for 90 min (Optima XPN-80, rotor 50.2 Ti, Beckman Coulter). The resulting supernatant was loaded onto a Ni Sepharose 6 Fast Flow resin column (5 ml of bed volume, GE Healthcare) equilibrated with buffer A. The protein-loaded column was washed and the bound protein was eluted with 100 mM imidazole. The protein fractions containing hAdxR with $A_{280}/A_{450} < 15$ were pooled, concentrated in an Amicon YM 30 concentrator and loaded onto a Superdex 75 16/60 column (GE-Healthcare) equilibrated with buffer B (20 mM Tris-HCl, pH 7.5, 100 mM NaCl, glycerol 5% (v/v)). The protein fractions containing hAdxR with A_{271}/A_{450} ~8 were pooled, the purity was monitored on Coomassie Blue SDS gel, and hAdxR was stored at −80 °C.

Expression and purification of mature recombinant Coq6p from Saccharomyces cerevisiae

Overexpression of *S. cerevisiae* Coq6pΔ1-24-MBP fusion protein was achieved by using BL21(DE3) *E. coli* strain co-transformed with pMAL-c2X-Coq6pΔ1-24 and pGro7. The cultures were grown in LB medium at 37 °C in the presence of glucose (0.2% w/v), ampicillin (100 μg/ml) and chloramphenicol (34 μg/ml). When A_{600nm} reached 0.6, chaperone expression was induced with L-arabinose (2 mg/ml). Temperature was then shifted to 18 °C for 30 min and IPTG was added to a final concentration of 0.15 mM. After overnight incubation at 18 °C, cells were harvested by centrifugation at 5000×*g* for 10 min. All subsequent operations were carried out at 4 °C. The cells were resuspended in 5 volumes of lysis buffer (50 mM Tris-HCl pH 7.5, 150 mM NaCl, glycerol 5%(v/v)), in the presence of cOmplete protease inhibitors (Roche). Cells were lysed by sonication with amplitude of 40% for 10 min, and then subjected to ultracentrifugation at 180,000×*g* for 90 min. The resulting supernatant was loaded onto an MBP-Trap HP column (GE Healthcare) equilibrated with buffer C (50 mM Tris-HCl pH 7.5, 150 mM NaCl, 1 mM EDTA, glycerol 5% (v/v)). Coq6pΔ1-24-MBP was eluted with a linear maltose gradient (0–20 mM) and loaded onto a HiLoad 26/600 Superdex 200 pg column (GE Healthcare) equilibrated with buffer C. The protein fractions corresponding to a dimer and a monomer of Coq6pΔ1-24-MBP were pooled and concentrated with Amicon Ultra 100 K columns (Millipore). The MBP tag was cleaved from the fusion protein by incubating the pooled fractions of Coq6pΔ1-24-MBP with FactorXa (New England Biolabs) with a 1:50 ratio. The cleaved MBP tag (42 kDa) was removed by using UnoQ1column (Bio-Rad) which binds to Coq6pΔ1-24 but not MBP. UnoQ1 column was equilibrated with buffer D (50 mM Tris-HCl pH 7.5, 20 mM NaCl, glycerol 5% (v/v)). Coq6pΔ1-24 was eluted with a NaCl linear gradient (0–400 mM). The purified protein was loaded onto a Superdex 200 10/300 GL and found to be >95% pure as judged by SDS-PAGE. Coq6pΔ1-24 was aliquoted and stored at −80 °C in 50 mM Tris-HCl, pH 7.5, 150 mM NaCl, glycerol 5% (v/v).

Expression and purification of mature recombinant Yah1p from Saccharomyces cerevisiae

Overexpression of *S. cerevisiae* Yah1pΔ1-57 was achieved by using BL21(DE3) *E. coli* strain transformed with pET15b-Yah1pΔ1-57. The cultures were grown in LB medium at 37 °C in the presence of ampicillin (100 μg/ml) until they reached $A_{600nm} = 0.6$. Temperature was then shifted to 25 °C and induced with IPTG to a final concentration of 0.75 mM. After overnight incubation at 25 °C, cells were harvested by centrifugation at 5000×*g* for 10 min. All subsequent operations were carried out at 4 °C. The cells were resuspended in 5 volumes of buffer E (50 mM Tris-HCl pH 7.5, 20 mM NaCl) in the presence of cOmplete protease inhibitors (Roche). Cells were lysed by sonication with amplitude of 40% for 10 min, and then subjected to ultracentrifugation at 180,000×*g* for 90 min. The resulting supernatant was loaded onto a UnoQ6 column equilibrated with buffer E, and the protein was eluted with a linear gradient of NaCl (0–500 mM). After concentration with an Amicon Ultra 5 K column (Millipore), Yah1pΔ1-57 was loaded onto a HiLoad 16/600Superdex 75 pg equilibrated with 25 mM Tris-HCl buffer, pH 7.5, 50 mM NaCl. The protein was pooled, aliquoted and stored at −80 °C.

UV-visible spectroscopic analysis

Absorption spectra were recorded on a Jasco V-630 UV Vis spectrophotometer apparatus equipped with a Peltier temperature controller. The extinction coefficient of the protein-bound flavin in hAdxR was determined spectrophotometrically quantitating the FAD released after SDS treatment.[44] A ~10 μM solution (1 mL) of hAdxR in 10 mM Tris-HCl buffer (pH 7.5) was incubated in the presence of 20 μL of a fresh solution of SDS 10% for 5 min. Denatured polypeptides were removed by centrifugation at 15,000 *g* for 15 min. The FAD concentration in the supernatant was determined using $\varepsilon_{450} = 11.3\ mM^{-1}cm^{-1}$. The protein concentration was determined by the Bradford method and confirmed by measuring the absorbance at 280 nm, corrected by the contribution of the flavin after denaturation with 0.1% SDS. Anaerobic titrations with NADPH/NADH were performed under N_2 atmosphere. An anaerobic solution containing hAdxR was placed in a 500 μL cuvette and the changes of spectra after each addition of NADPH/NADH were recorded. The concentration of NADPH/NADH solution was spectrophotometrically determined ($\varepsilon_{340\ nm} = 6.22\ cm^{-1}mM^{-1}$).

Steady-state enzyme assays

The NAD(P)H-ferricyanide diaphorase activity tests were performed in 100 mM Tris-HCl buffer (pH 7.5) at 25 °C with $K_3[Fe(CN)_6]$ ($\Delta\varepsilon_{420\ nm} = 1.02\ cm^{-1}mM^{-1}$) as electron acceptor. The reaction mixtures (0.5 mL) contained 1 mM $K_3[Fe(CN)_6]$, 1 μM–2 mM NAD(P)H and 30 nM hAdxR.

Stopped-flow kinetic studies

All stopped-flow experiments were conducted on a Hi-Tech TGK Scientific SF-61 DX2 stopped-flow absorbance spectrophotometer equipped with a temperature-controlled circulating water bath at 25 °C. In order to avoid the slow re-oxidation of $FADH_2$ by O_2 during experiments, the stopped-flow instrument flow system was made anaerobic by overnight incubation with an oxygen scrubbing solution consisting of 200 μM protocatechuic acid (PCA) and 0.1 unit/ml protocatechuate dioxygenase (PCD).[45] Prior to performing the stopped-flow experiments, enzyme and substrate solutions were degassed into a nitrogen atmosphere in the glovebox (MBraun) and transferred to anaerobic syringes and the oxygen-

scrubbing system (PCA/PCD) was added to all solutions, as described above. Stopped-flow studies of the reductive half-reaction catalyzed by hAdxR were performed by rapid mixing of hAdxR (12.5–25 μM) with an equal volume of either NADH or NADPH (ranging from 12.5 μM to 1.6 mM). Reactions were performed in 100 mM Tris-HCl buffer, pH 7.5 in the absence of $MgCl_2$ and in 100 mM sodium phosphate buffer, pH 7.5 in the presence of $MgCl_2$. The changes in absorbance at 450, 530, and 700 nm were followed in single wavelength modes. Triplicate measurements differed typically by less than 5%. Triplicates traces were fit to Eq 1 with KinetAsyst software to obtain observed rate constants (k_{obs}) and the corresponding amplitude (A). In Eq 1, Abs(t) is A at time t, i the number of transient phases, A_i and $k_{obs(i)}$ correspond to the amplitude and rate constant for the i^{th} transient phase, and C is the offset. Observed rate constants were then fit to Eq 2 as a function of [NADPH] or [NADH] ([S]) to yield the maximum observed rate constant (k_{max}) and the [S] at half maximal k_{obs} or apparent K_d.

$$\mathrm{Abs(t)} = \sum_{i}^{n} \mathrm{A_i}\ e^{-k_{obs(i)}t} + \mathrm{C} \quad (1)$$

$$k_{obs(i)} = \frac{k_{max(i)}[S]}{K_{d(i)} + [S]} \quad (2)$$

Funding and additional information

We acknowledge acknowledge support the "Initiative d'Excellence" program from the French State (Labex program "DYNAMO", ANR-11-LABX-0011-01) and the "ANR PRC program" from the French State (PHEYDR ANR-23-CE44-0015-01) . This work was supported by Collège de France, the Centre National de la Recherche Scientifique and Sorbonne Université.

Supporting Information

S1. Alphafold Model of hAdxR **S2**. cDNA and protein sequence of human mature hAdxR cloned into pETDuet-1; **S3**. Purification and biochemical characterization of recombinant hAdxR; **S4**. Kinetics trace at 450 nm of re-oxidation of the reduced flavin of hAdxR; **S5**. Effect of $MgCl_2$ on the K_m of hAdxR for NADPH; Effect of $MgCl_2$ on the K_m of hAdxR for NADPH; **S6**. DNA and protein sequence of Coq6p from *Saccharomyces cerevisiæ* cloned into pMalc2X; **S7**. Purification and biochemical characterization of mature recombinant Coq6p Δ1-24 from *Saccharomyces cerevisae*; **S8**. DNA sequence of Yah1pΔ1-57 from *Saccharomyces cerevisiæ* cloned into pET15b; **S9**. Purification and biochemical characterization of mature recombinant Yah1p from *Saccharomyces cerevisiae*. **S10**. Sequence alignments of AdxR with homologs of different species. **S11**. Kinetics of reduction of Coq6p by the electron transfer chain NADPH-hAdxR-Yah1p-Coq6p. **S12**. Substrates of Coq6p, zeaxanthin epoxidase, and squalene monooxygenase, three proteins receiving reducing equivalents from an electron transfer chain.

Abbreviations

AdxR	(adrenodoxin reductase)
CT	(charge transfer)
CYPOR	(cytochrome P450 oxidoreductase).
FAD	(Flavin adenine dinucleotide)
FdxR	(ferredoxin reductase)
Fdx1	(ferredoxin 1)
Fdx2	(ferredoxin 2)
FNR	(ferredoxin NADP + reductase)
GR	(glutathione reductase)
HPLC	(high performance liquid chromatography)
IPTG	(isopropyl ß-D-thiogalactopyranoside)
ROS	(reactive oxygen species)
MBP	(maltose binding protein)
NADH	(nicotinamide adenine dinucleotide, reduced form)
NAD +	(nicotinamide adenine dinucleotide, oxidized form)
NADPH	(nicotinamide adenine dinucleotide phosphate, reduced form)
NAD +	(nicotinamide adenine dinucleotide phosphate, oxidized form)
NOS	(NO synthase)
PCA	(protocatechuic acid)
PCD	(protocatechuate dioxygenase)
SEC-MALS	(size-exclusion chromatography–multi-angle light scattering)
SDS-PAGE	(sodium dodecyl sulfate–polyacrylamide gel electrophoresis)
TdR	(thioredoxin reductase)

Author Contributions

M. L., D. H., conceptualization; L. G., S. T. V., B. F., M. L., D. H. investigation; M. L., D. H. formal analysis; M. L., D. H., F. P., M. F., writing and reviewing; M. F. funding acquisition.

Acknowledgements

We gratefully acknowledge Ulli Mühlenhoff for providing the pET-duet plasmid overexpressing hAdxR and Yah1p.

Conflict of Interests

The authors declare that they have no conflicts of interest with the contents of this article.

Data Availability Statement

The data that support the findings of this study are available from the corresponding author upon reasonable request.

Keywords: adrenodoxin reductase · Arh1 · coenzyme Q · Coq6p · electron transfer · ferredoxin · ferredoxin reductase · flavin · hydride transfer · kinetics · magnesium chloride · spectrophotometry · stopped-flow · pyridine nucleotide · Yah1p

[1] a) Y. Wang, S. Hekimi, *Trends Endocrinol. Metab.* **2019**, *30*, 929–943; b) L. Fernandez-Del-Rio, C. F. Clarke, *Metabolites* **2021**, *11*; c) R. M. Guerra, D. J. Pagliarini, *Trends Biochem. Sci.* **2023**, *48*, 463–476.
[2] R. K. Behan, S. J. Lippard, *Biochemistry* **2010**, *49*, 9679–9681.
[3] a) M. Ozeir, U. Muhlenhoff, H. Webert, R. Lill, M. Fontecave, F. Pierrel, *Chem. Biol.* **2011**, *18*, 1134–1142; b) A. Ismail, V. Leroux, M. Smadja, L. Gonzalez, M. Lombard, F. Pierrel, C. Mellot-Draznieks and M. Fontecave, *PLoS Comput. Biol.* **2016**, *12*, e1004690.
[4] F. Pierrel, O. Hamelin, T. Douki, S. Kieffer-Jaquinod, U. Muhlenhoff, M. Ozeir, R. Lill, M. Fontecave, *Chem. Biol.* **2010**, *17*, 449–459.
[5] a) E. Romero, J. R. Gomez Castellanos, G. Gadda, M. W. Fraaije, A. Mattevi, *Chem. Rev.* **2018**, *118*, 1742–1769; b) C. E. Paul, D. Eggerichs, A. H. Westphal, D. Tischler, W. J. H. van Berkel, *Biotechnol. Adv.* **2021**, *51*, 107712; c) K. Crozier-Reabe, G. R. Moran, *Int. J. Mol. Sci.* **2012**, *13*, 15601–15639.
[6] H. Webert, S. A. Freibert, A. Gallo, T. Heidenreich, U. Linne, S. Amlacher, E. Hurt, U. Muhlenhoff, L. Banci, R. Lill, *Nat. Commun.* **2014**, *5*, 5013.
[7] a) P. A. Karplus, C. M. Bruns, *J. Bioenerg. Biomembr.* **1994**, *26*, 89–99; b) A. Aliverti, V. Pandini, A. Pennati, M. de Rosa, G. Zanetti, *Arch. Biochem. Biophys.* **2008**, *474*, 283–291.
[8] W. L. Miller, *Endocrinology* **2005**, *146*, 2544–2550.
[9] M. Medina, *FEBS J.* **2009**, *276*, 3942–3958.
[10] R. C. Rohrich, N. Englert, K. Troschke, A. Reichenberg, M. Hintz, F. Seeber, E. Balconi, A. Aliverti, G. Zanetti, U. Kohler, M. Pfeiffer, E. Beck, H. Jomaa, J. Wiesner, *FEBS Lett.* **2005**, *579*, 6433–6438.
[11] a) R. Lill, U. Muhlenhoff, *Annu. Rev. Cell Dev. Biol.* **2006**, *22*, 457–486; b) V. Schulz, S. Basu, S. A. Freibert, H. Webert, L. Boss, U. Muhlenhoff, F. Pierrel, L. O. Essen, D. M. Warui, S. J. Booker, O. Stehling, R. Lill, *Nat. Chem. Biol.* **2023**, *19*, 206–217.
[12] a) P. M. Hwang, F. Bunz, J. Yu, C. Rago, T. A. Chan, M. P. Murphy, G. F. Kelso, R. A. Smith, K. W. Kinzler, B. Vogelstein, *Nat. Med.* **2001**, *7*, 1111–1117; b) G. Liu, X. Chen, *Oncogene* **2002**, *21*, 7195–7204; c) A. Bhaduri, A. Ungewickell, L. D. Boxer, V. Lopez-Pajares, B. J. Zarnegar, P. A. Khavari, *Dev. Cell* **2015**, *35*, 444–457.
[13] Y. Zhang, Y. Qian, J. Zhang, W. Yan, Y. S. Jung, M. Chen, E. Huang, K. Lloyd, Y. Duan, J. Wang, G. Liu, X. Chen, *Genes Dev.* **2017**, *31*, 1243–1256.
[14] A. Paul, A. Drecourt, F. Petit, D. D. Deguine, C. Vasnier, M. Oufadem, C. Masson, C. Bonnet, S. Masmoudi, I. Mosnier, L. Mahieu, D. Bouccara, J. Kaplan, G. Challe, C. Domange, F. Mochel, O. Sterkers, S. Gerber, P. Nitschke, C. Bole-Feysot, L. Jonard, S. Gherbi, O. Mercati, I. Ben Aissa, S. Lyonnet, A. Rotig, A. Delahodde, S. Marlin, *Am. J. Hum. Genet.* **2017**, *101*, 630–637.
[15] L. E. Vickery, *Steroids* **1997**, *62*, 124–127.
[16] a) A. V. Grinberg, F. Hannemann, B. Schiffler, J. Muller, U. Heinemann, R. Bernhardt, *Proteins* **2000**, *40*, 590–612; b) K. M. Ewen, M. Kleser, R. Bernhardt, *Biochim. Biophys. Acta* **2011**, *1814*, 111–125.
[17] a) K. Inouye, T. Sakaki, *Biotechnol. Annu. Rev.* **2001**, *7*, 179–194; b) K. M. Ewen, M. Ringle, R. Bernhardt, *IUBMB Life* **2012**, *64*, 506–512.
[18] J. Li, S. Saxena, D. Pain, A. Dancis, *J. Biol. Chem.* **2001**, *276*, 1503–1509.
[19] a) H. Lange, A. Kaut, G. Kispal, R. Lill, *Proc. Natl. Acad. Sci. USA* **2000**, *97*, 1050–1055; b) Y. Shi, M. Ghosh, G. Kovtunovych, D. R. Crooks, T. A. Rouault, *Biochim. Biophys. Acta* **2012**, *1823*, 484–492.
[20] a) M. H. Barros, F. G. Nobrega, A. Tzagoloff, *J. Biol. Chem.* **2002**, *277*, 9997–10002; b) M. H. Barros, C. G. Carlson, D. M. Glerum, A. Tzagoloff, *FEBS Lett.* **2001**, *492*, 133–138; c) A. D. Sheftel, O. Stehling, A. J. Pierik, H. P. Elsasser, U. Muhlenhoff, H. Webert, A. Hobler, F. Hannemann, R. Bernhardt, R. Lill, *Proc. Natl. Acad. Sci. USA* **2010**, *107*, 11775–11780.
[21] a) P. R. Joshi, S. Sadre, X. A. Guo, J. G. McCoy, V. K. Mootha, *J. Biol. Chem.* **2023**, *299*, 105075; b) M. B. Dreishpoon, N. R. Bick, B. Petrova, D. M. Warui, A. Cameron, S. J. Booker, N. Kanarek, T. R. Golub, P. Tsvetkov, *J. Biol. Chem.* **2023**, *299*, 105046.
[22] M. Zulkifli, A. U. Okonkwo, V. M. Gohil, *J. Mol. Biol.* **2023**, *435*, 168317.
[23] a) K. Suhara, Y. Ikeda, S. Takemori, M. Katagiri, *FEBS Lett.* **1972**, *28*, 45–47; b) J. W. Chu, T. Kimura, *J. Biol. Chem.* **1973**, *248*, 5183–5187; c) J. W. Chu, T. Kimura, *J. Biol. Chem.* **1973**, *248*, 2089–2094.
[24] a) Y. Sagara, A. Wada, Y. Takata, M. R. Waterman, K. Sekimizu, T. Horiuchi, *Biol. Pharm. Bull.* **1993**, *16*, 627–630; b) C. Vonrhein, U. Schmidt, G. A. Ziegler, S. Schweiger, I. Hanukoglu, G. E. Schulz, *FEBS Lett.* **1999**, *443*, 167–169.
[25] K. Ishimura, H. Fujita, *Microsc. Res. Tech.* **1997**, *36*, 445–453.
[26] a) G. A. Ziegler, C. Vonrhein, I. Hanukoglu, G. E. Schulz, *J. Mol. Biol.* **1999**, *289*, 981–990; b) G. A. Ziegler, G. E. Schulz, *Biochemistry* **2000**, *39*, 10986–10995.
[27] J. J. Muller, A. Lapko, G. Bourenkov, K. Ruckpaul, U. Heinemann, *J. Biol. Chem.* **2001**, *276*, 2786–2789.
[28] Y. Nonaka, T. Sugiyama, T. Yamano, *J. Biochem.* **1982**, *92*, 1693–1701.
[29] F. Fischer, D. Raimondi, A. Aliverti, G. Zanetti, *Eur. J. Biochem.* **2002**, *269*, 3005–3013.
[30] K. J. McLean, N. S. Scrutton, A. W. Munro, *Biochem. J.* **2003**, *372*, 317–327.
[31] M. Sabri, A. J. Dunford, K. J. McLean, R. Neeli, N. S. Scrutton, D. Leys, A. W. Munro, *Biochem. J.* **2009**, *417*, 103–112.
[32] M. E. Brandt, L. E. Vickery, *Arch. Biochem. Biophys.* **1992**, *294*, 735–740.
[33] J. I. Pedersen, H. K. Godager, *Biochim. Biophys. Acta* **1978**, *525*, 28–36.
[34] J. D. Lambeth, H. Kamin, *J. Biol. Chem.* **1976**, *251*, 4299–4306.
[35] S. Baroni, V. Pandini, M. A. Vanoni, A. Aliverti, *Biochemistry* **2012**, *51*, 3819–3826.
[36] a) R. Tao, Y. Zhao, H. Chu, A. Wang, J. Zhu, X. Chen, Y. Zou, M. Shi, R. Liu, N. Su, J. Du, H. M. Zhou, L. Zhu, X. Qian, H. Liu, J. Loscalzo, Y. Yang, *Nat. Methods* **2017**, *14*, 720–728; b) Y. Zhao, Y. Yang, J. Loscalzo, *Methods Enzymol.* **2014**, *542*, 349–367; c) V. Cracan, D. V. Titov, H. Shen, Z. Grabarek, V. K. Mootha, *Nat. Chem. Biol.* **2017**, *13*, 1088–1095.
[37] a) K. Knight, N. S. Scrutton, *Biochem. J.* **2002**, *367*, 19–30; b) O. Roitel, N. S. Scrutton, A. W. Munro, *Biochemistry* **2003**, *42*, 10809–10821; c) S. Daff, *Biochemistry* **2004**, *43*, 3929–3932.
[38] D. E. Draper, D. Grilley, A. M. Soto, *Annu. Rev. Biophys. Biomol. Struct.* **2005**, *34*, 221–243.
[39] A. Pennati, G. Zanetti, A. Aliverti, G. Gadda, *Biochemistry* **2008**, *47*, 3418–3425.
[40] A. M. Romani, *Arch. Biochem. Biophys.* **2011**, *512*, 1–23.
[41] S. K. Aulakh, S. J. Varma, M. Ralser, *Curr. Opin. Genet. Dev.* **2022**, *77*.
[42] F. Bouvier, A. d'Harlingue, P. Hugueney, E. Marin, A. Marion-Poll, B. Camara, *J. Biol. Chem.* **1996**, *271*, 28861–28867.
[43] a) B. P. Laden, Y. Tang, T. D. Porter, *Arch. Biochem. Biophys.* **2000**, *374*, 381–388; b) L. Li, T. D. Porter, *Arch. Biochem. Biophys.* **2007**, *461*, 76–84.
[44] A. Aliverti, B. Curti, M. A. Vanoni, *Methods Mol. Biol.* **1999**, *131*, 9–23.
[45] P. V. Patil, D. P. Ballou, *Anal. Biochem.* **2000**, *286*, 187–192.

Manuscript received: October 26, 2023
Revised manuscript received: December 22, 2023
Accepted manuscript online: December 23, 2023
Version of record online: February 2, 2024